

文章编号: 1000-4734(2017)01-0016-13

广西八渡金矿床含金硫化物矿物学 与地球化学研究

董文斗^{1,2*}, 苏文超^{1*}, 沈能平¹, 朱路艳^{1,2}, 蔡佳丽¹

(1. 中国科学院 地球化学研究所 矿床地球化学国家重点实验室, 贵州 贵阳 550081; 2. 中国科学院大学, 北京 100049)

摘要: 广西田林县八渡金矿床主要产于辉绿岩侵入体中, 广泛发育乳白色石英网脉, 蚀变辉绿岩体即为金矿体, 具有硅化、粘土化、碳酸盐化和硫化物化等卡林型金矿热液蚀变特征。本文采用电子探针 (EPMA) 背散射电子图像 (BSE)、波谱 (WDS) 和能谱 (EDS) 分析技术, 对该矿床原生矿石中含金硫化物显微岩相学结构以及主量和微量元素含量和分布规律进行了系统研究, 认为金主要是以不可见化学结合态金 (Au^+) 的形式赋存于含砷黄铁矿和毒砂之中。含金硫化物与热液交代形成的金红石密切共生, 并保留含钛铁辉石或钛铁矿等矿物的假象, 金红石的形成是辉绿岩中含钛铁辉石或钛铁矿热液蚀变的产物, 含金硫化物形成所需要的 Fe 来自辉绿岩中含钛辉石或钛铁矿等矿物的溶解, Fe 的硫化物化过程是导致含金硫化物形成的重要机制。

关键词: 桂西北; 辉绿岩; 金矿床; 黄铁矿; 毒砂

中图分类号: P571; P595

文献标识码: A

doi: 10.16461/j.cnki.1000-4734.2017.01.003

作者简介: 董文斗, 男, 1989 年生, 博士研究生, 主要从事矿床地球化学研究. E-mail: dongwendou@mail.gyig.ac.cn

Mineralogy and geochemistry of gold-bearing sulfides in Badu gold deposit, Guangxi Province, China

DONG Wen-dou^{1,2}, SU Wen-chao¹, SHEN Neng-ping¹, ZHU Lu-yan^{1,2}, CAI Jia-li¹

(1. State Key Laboratory of Ore Deposit Geochemistry, Institute of Geochemistry, Chinese Academy of Sciences, Guiyang 550081, China; 2. University of Chinese Academy of Sciences, Beijing 100049, China)

Abstract: Badu gold deposit mainly occurs within diabase intrusions in Tianlin County, Guangxi Province, China. It hosts within altered gabbro diabase, with intensive barren milky quartz veins and veinlets. The alteration related to mineralization caused silicification, argillization, carbonatization and sulfidation of gabbro diabase. In this paper, electron probe microanalysis (EPMA), backscattered electron image (BSE), wavelength dispersive spectrometer (WDS) and energy dispersive spectrometer (EDS) analyses were used to observe petrographic texture and determine element contents and distributions of S, Fe, Au, As and etc., in gold-bearing sulfides of Badu gold deposit. Results show that gold mainly occurs as invisible chemical bonding (Au^+) in the forms of arsenian pyrite and arsenopyrite. The gold-bearing sulfides occur with the hydrothermal rutile indicative the products of Ti-bearing clinopyroxene and ilmenite. Iron in sulfide minerals is probably derived from

收稿日期: 2015-04-09

基金项目: 国家重点基础研究发展计划 973 课题 (编号: 2014CB440904); 国家自然科学基金项目 (编号: 41272113); 矿床地球化学国家重点实验室领域前沿项目 (编号: 201104); 矿床地球化学国家重点实验室“十二五”项目群 (编号: SKLOGD-ZY125-01)

* 通讯作者, E-mail: suwenchao@vip.gyig.ac.cn

dissolution of Ti-bearing clinopyroxene and ilmenite in the diabase, sulfidized by H_2S -rich fluids to precipitate gold-bearing arsenian pyrite and arsenopyrite.

Keywords: Guangxi Province; diabase; gold deposit; pyrite; arsenopyrite

国内外大量研究表明,含砷黄铁矿和毒砂是卡林型金矿原生矿石中最重要的载金矿物,金主要以“不可见金”的形式赋存于含砷黄铁矿和毒砂之中^[1-6]。滇黔桂“金三角”是我国著名的卡林型金矿集区之一,矿体主要产于沉积岩之中(如水银洞、丫他和烂泥沟等)。近年来在桂西北地区发现一种产于辉绿岩中的金矿床(如八渡等)^[7-9],甚至在同一矿区(如者桑等)金矿体既产于沉积岩中,又产于辉绿岩体之中。前人对这类金矿床的地质特征、成矿流体及其成矿预测等进行了初步研究^[10-17],但对这类金矿床含金硫化物矿物学与地球化学特征及其金的赋存状态等研究较少。本文采用电子探针分析技术,对八渡金矿床含金硫化物显微岩相学结构、载金矿物的矿物学与地球化学等进行了系统研究,为进一步探讨该类型金矿床的成因提供理论依据。

1 区域地质概况

研究区地处南华准地台右江再生地槽桂西坳陷西林-百色断褶带中,位于古特提斯构造域和滨太平洋的复合域内,它们联合控制了本区构造特征及演化历史。该区特殊的大地构造背景,导致了构造的复杂性和多期基性岩浆活动^[18]。

区域上出露地层有中、上寒武统和泥盆系-下、中三叠统及第三系。其中,中、上寒武统仅在隆林、德峨和蛇场等地出露,岩性主要为碳酸盐岩,底部夹碎屑岩。泥盆系出露于八渡背斜的轴部,下统为碎屑岩,中、上统主要为碳酸盐岩。石炭系、二叠系分布于八渡背斜翼部,岩性主要为碳酸盐岩,局部地区少数层位为硅质岩、火山碎屑沉积岩(图1)。三叠系分布广泛,绝大部分为碎屑岩岩相,仅下统为碳酸盐岩、碎屑岩交互相;中三叠统发育浊积岩,是本区最重要的赋金层位。第三系仅见于新生代断陷盆地中,岩性为杂色复陆屑建造。

区域上断裂、褶皱发育,构造复杂。构造线以北西向为主,在西林、隆林一带向北西西弯转,呈帚状或弧形构造;乐业、凌云“S”形构造走向近于南北。褶皱呈紧密线状,构成大型右

江复式向斜,次级褶皱具尖棱状、拱状特点,地层倾角一般 $40^\circ \sim 60^\circ$,断裂附近 $70^\circ \sim 80^\circ$,局部直立或倒转。区域大断裂田林-巴马隐伏深断裂和右江大断裂影响着本区地质构造的发生与发展。前者控制晚古生代沉积岩相和厚度变化;后者切割寒武系-第三系,破坏复式向斜轴部,控制第三纪盆地的形成与展布。次级断裂以北西-北西西向为主,北北东、北北西仅局部分布,延伸不远,形成较晚。

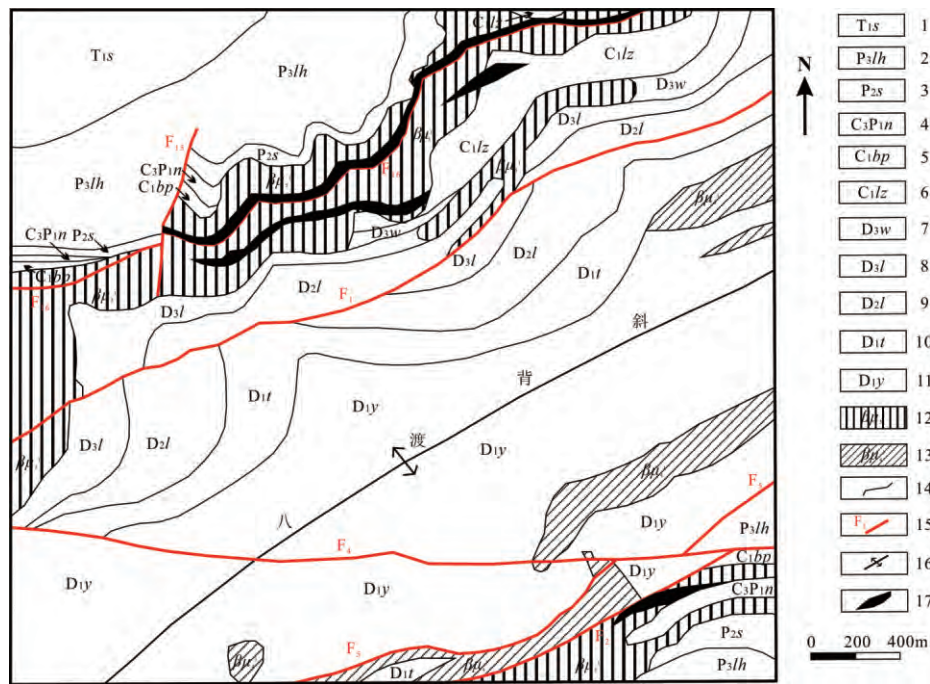
区域岩浆岩零星分布于隆林、西林、田林、百色、巴马一带,主要为印支期海底喷发或顺层侵入的基性-超基性岩。另外于巴马、凌云一带有少许燕山期酸性花岗斑岩脉、石英斑岩脉。

2 矿床地质特征

广西田林县八渡金矿床位于右江再生地槽西林-百色断褶带南部的八渡背斜轴部,矿体产于辉绿岩体内部或与下泥盆统郁江组(D_{1y})接触带蚀变岩中(图1),矿体长约数十米至数百米不等,呈透镜状,金矿体中发育石英细网脉^[19],与典型沉积岩容矿的卡林型金矿床^[20]类似,大量石英脉的出现暗示了强烈的硅化,提供流体运移的通道,流体-围岩交代反应而沉淀出金。

矿区内地层从泥盆系-三叠系均有出露。其中,泥盆系地层出露于八渡背斜轴部,岩性主要为碎屑岩、硅质岩和碳酸盐岩;石炭系地层分布于八渡背斜的核部,上石炭统-下二叠统岩性主要为硅质岩和碳酸盐岩;二叠系地层分布于八渡背斜的翼部,岩性主要为灰岩及硅质岩;三叠系地层在本区外围分布广泛,绝大部分为碎屑岩岩相,仅下统为碳酸盐岩、碎屑岩交互相。

矿区内褶皱以八渡背斜为主,其为一长轴状褶皱,轴向北东,枢纽起伏,并向两端倾伏。背斜核部出露最老地层为下泥盆统郁江组(D_{1y}),翼部依次为下泥盆统塘丁组(D_{1t})-下三叠统石炮组(T_{1s})。八渡背斜的北翼岩层倾向北西,倾角一般为 $30^\circ \sim 50^\circ$,南翼岩层倾向南东,倾角一般为 $30^\circ \sim 40^\circ$,为一轴面近于直立的对称褶皱。但由于断裂发育,区域性大断裂均通过背斜区,



1-下三叠统石炮组; 2-上二叠统领导组; 3-中二叠统四大寨组; 4-上石炭-下二叠统南丹组; 5-下石炭统巴平组; 6-下石炭统鹿寨组; 7-上泥盆统五指山组; 8-上泥盆统榴江组; 9-中泥盆统罗富组; 10-下泥盆统塘丁组; 11-下泥盆统郁江组; 12-印支期辉绿岩; 13-华力西期辉绿岩; 14-地层界线; 15-断层及编号; 16-背斜轴; 17-金矿体

图 1 广西八渡金矿床地质简图 (据覃少耀和颜小东^[18]修改)

Fig. 1. Simplified geological map of Badu gold deposit in Guangxi Province, China (modified after Qin and Yan^[18]).

致使地层缺失, 岩层产状零乱(图 1)。矿区内主要为北东向断裂, 规模大, 破碎带发育, 围岩蚀变矿化较强, F_2 、 F_{16} 和两期辉绿岩形成与矿体走向一致的构造-岩浆岩带, 明显控制矿体的产出与展布, 力学性质以张扭性为主, 其走向长、断距大、破碎带宽; 破碎带几乎全部硅化, 发育构造石英岩、硅化构造角砾岩。矿区断裂具多次继承性活动, 并控制热液活动, 为主要的赋矿、容矿构造。

矿区出露的岩浆岩主要为基性辉绿岩及少量玄武岩, 沿八渡背斜轴部及断裂带, 基性浅成侵入岩发育, 形成多期次岩体, 呈带状分布。根据岩浆岩的成因和各岩相之间的先后关系进一步分为塘丁期喷出相玄武岩、华力西期次火山侵入相辉绿岩、印支期侵入相辉绿岩^[18]。塘丁期喷出相玄武岩分布于八渡背斜两翼的下泥盆统塘丁组, 分布范围极小且不连续, 遭受华力西期辉绿岩侵蚀, 岩体形态不清晰。华力西期辉绿岩分布于八渡背斜核部, 呈似层状侵入于下泥盆统郁江组和塘丁组, 由斜长石假晶及钠长石、辉石假

晶、金红石、板钛矿、榍石和锐钛矿等矿物组成。印支期辉绿岩侵入于下泥盆统郁江组-下三叠统地层和华力西期辉绿岩中, 分布范围广泛, 多沿北东向断裂展布, 主要呈岩床状或岩株状产出, 相对于华力西期辉绿岩, 它的侵入时间较晚, 其岩石种类主要属于细粒辉绿岩和中粒辉绿岩, 由含钛普通辉石、斜长石、普通角闪石、钛铁矿、磁铁矿、黑云母、磷灰石、榍石、黄铁矿等矿物组成^[18]。印支期辉绿岩与金矿化关系密切, 是本区金矿体的主要赋矿岩石(图 2)。

3 样品与分析方法

3.1 样品特征

八渡金矿床的原生矿石主要呈浅灰色块状, 以含石英脉和富含硫化物为主要特征(图 3A), 伴随有不同程度的硅化。对矿石切片进行观察发现, 硫化物以黄铁矿和毒砂为主, 大多呈浸染状分布, 颗粒较小(图 3B), 有石英-方解石脉切穿的部位硫化物质量分数很高。黄铁矿主要为自形-半自形立方体状、五角十二面体、八面体及其

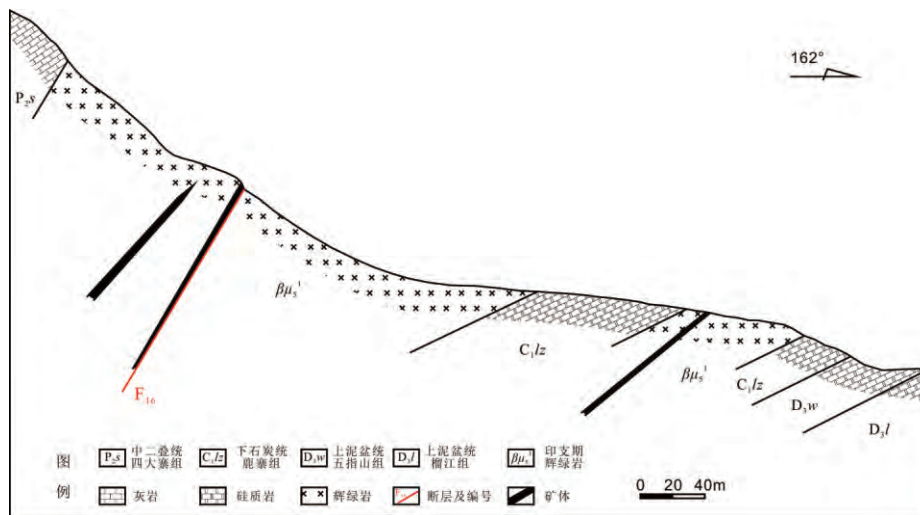


图 2 广西八渡金矿床地质剖面图

Fig. 2. Geological cross section of Badu gold deposit in Guangxi

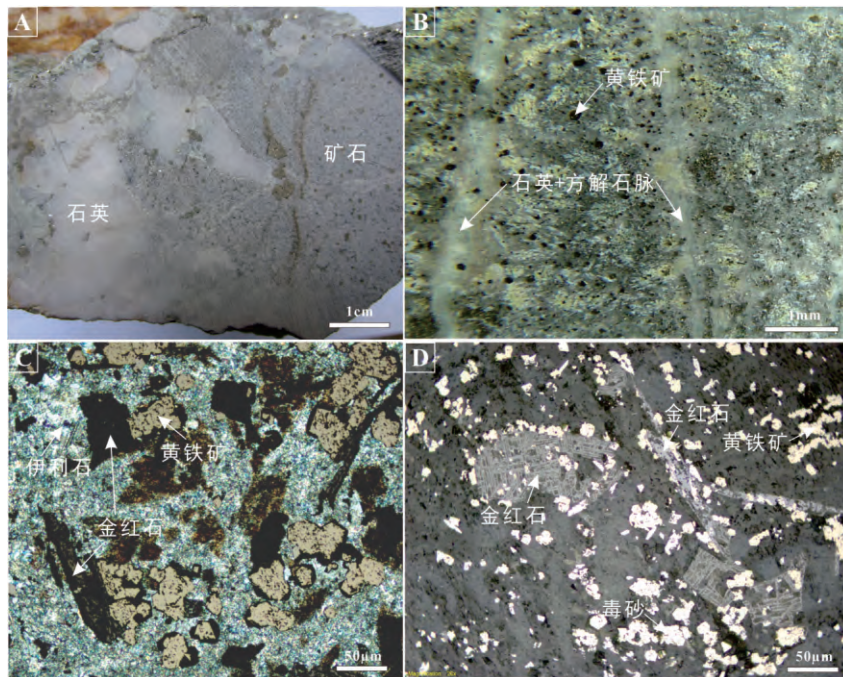


图 3 广西八渡金矿床矿石手标本照片及镜下显微照片

Fig. 3. Photograph and photomicrograph of ores from Badu gold deposit in Guangxi

聚形（近圆形），无环带，为热液成因黄铁矿（图 3 C, D）。透射偏光显微镜下发现有不同形态的金红石与黄铁矿密切共生，还富含伊利石等粘土矿物（图 3C）。图 3D 中背散射图像可见有大量针状或长柱状毒砂，呈浸染状围绕金红石分布，三种不同形态的金红石可能是由辉绿岩中不同的矿物蚀变，保留原矿物的晶体格架：右上方的长条状金红石由板状钛铁矿蚀变，靠左位置的网格状金红石由角闪石蚀变，保留角闪石的两

组解理，右下角位置的立方体状金红石由辉石蚀变，保留两组近垂直的解理。

3.2 分析方法

本次研究的样品产自八渡背斜南东翼，印支期辉绿岩与 F₂ 断层接触带中的矿体。将矿石样品磨制探针片，在系统显微岩相学研究的基础上，采用电子探针背散射电子图像（BSE）、波谱（WDS）和能谱（EDS）分析技术，对八渡金

矿床原生矿石中含金硫化物首先进行详细的镜下显微岩相学观察与描述,然后用电子探针对其中主量和微量(S、Fe、Au和As等)元素的质量分数及分布规律进行系统的研究。本次测试是在中国科学院地球化学研究所矿床地球化学国家重点实验室电子探针实验室完成的,所用仪器为日本岛津EPMA-1600型电子探针仪,EDAX公司的Genesis能谱仪和波谱仪用于测定黄铁矿和毒砂中的As、S、Fe和Au等元素的质量分数,S和Hg的检测限为0.05%,Fe、As、Ag、Au、Ni、Co、Sb和Te的检测限为0.03%,Se的检测限为0.01%。测试条件①能谱仪(EDS):加速电压为25 kV,束流为4 nA;②波谱仪(WDS):25 kV,10 nA测定Fe、S和As等元素;25 kV,40 nA测定Au,束斑大小为1 μm 。

4 测试结果与分析

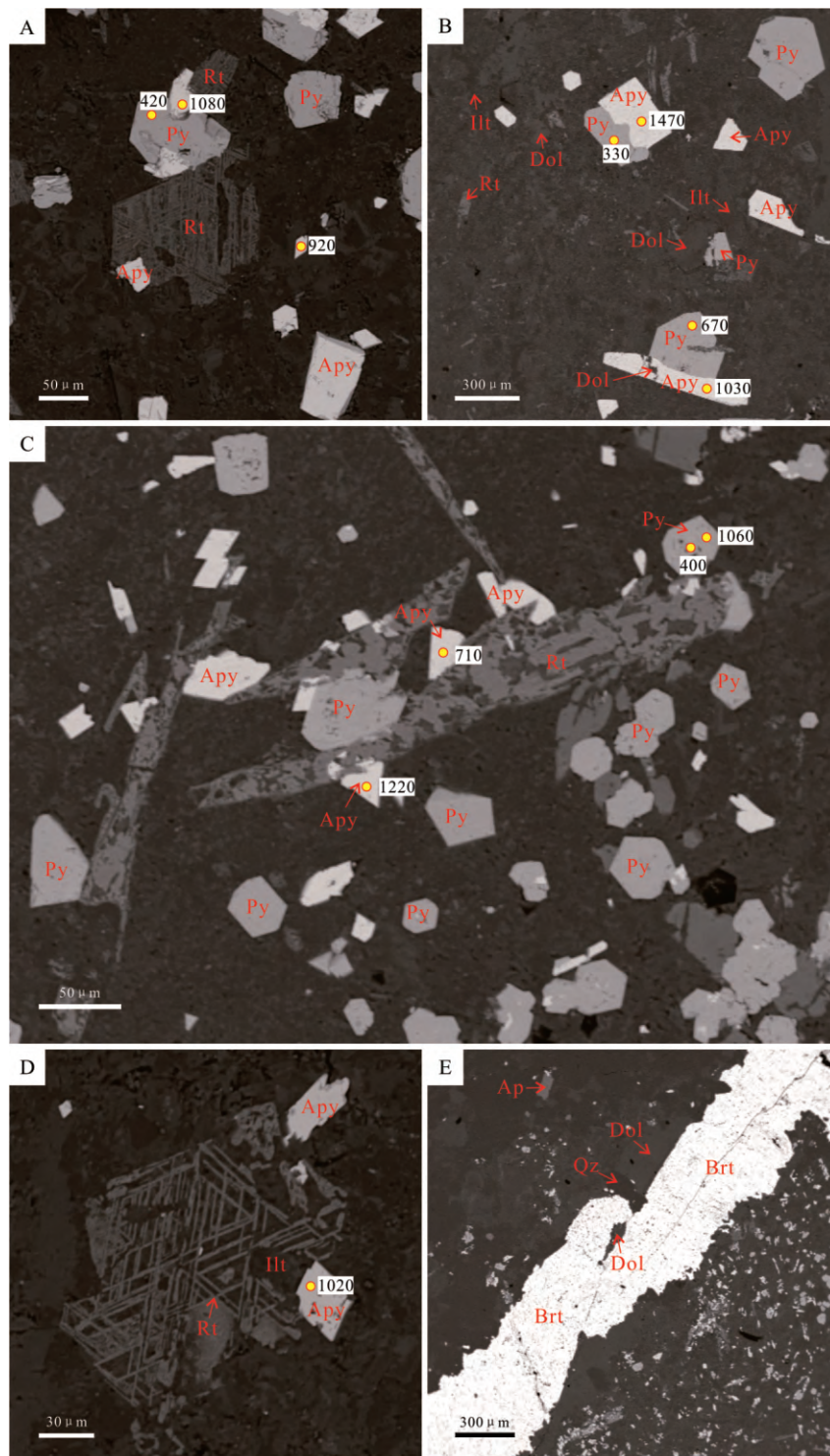
显微镜下观察和鉴定发现,黄铁矿和毒砂是八渡金矿床最主要的金属矿物。从电子探针背散射图像(BSE)(图4)可以看出,载金黄铁矿主要以细粒自形黄铁矿为主,常呈立方体、五角十二面体,粒径大小不等,主要集中于30~200 μm ,未见类似水银洞金矿床中黄铁矿的富砷环带^[21,22]。载金毒砂常呈菱形、长柱状、矛头状等自形晶,粒径大小不等,主要集中于20~100 μm 。能谱(EDS)分析显示,大部分载金黄铁矿和毒砂围绕着金红石分布(图4A、C),金红石主要有粒状(图4A、D)和长条状(图4C)两种形态,其中粒状金红石呈钛铁矿晶体格架。金红石内部的空隙中充填着伊利石等粘土矿物(图4D)。此外,矿石中还见到重晶石脉,微细磷灰石,石英,白云石等脉石矿物(图4E)。围岩蚀变主要有硅化、黄铁矿化、毒砂化、碳酸盐化、重晶石化、伊利石化等。

对含金硫化物-黄铁矿和毒砂进行波谱(WDS)点分析,测试结果和检测限列于表1和表2,黄铁矿和毒砂总共测得175个有效点中,有81个测点的金质量分数高于检出限(300×10^{-6})。其中,黄铁矿中Fe和S的质量分数分别在42.2%~46.1%和47.2%~53.5%之间,91个测点中有44个测点的金质量分数高于检出限,其Au质量分数在 310×10^{-6} ~ 1680×10^{-6} 之间,平均质量分数为 593×10^{-6} 。值得一提的是,这类黄

铁矿中As质量分数较高(0.56%~9.16%,平均质量分数为3.35%),应属含砷黄铁矿。含砷黄铁矿中的Au质量分数随着黄铁矿颗粒的减小而增加^[23],本次研究中也同样发现小颗粒的含砷黄铁矿有更高质量分数的金,因而在较大颗粒上的测点中金质量分数往往低于检测限。毒砂中Fe和S的质量分数分别在32.2%~35.2%和20.4%~25.8%之间,84个测点中有37个测点的金质量分数高于检出限,其Au质量分数在 300×10^{-6} ~ 1470×10^{-6} 之间,平均质量分数 593×10^{-6} ,该类毒砂中As质量分数在39.6%~47.1%之间,平均质量分数为44.0%,略低于毒砂的As质量分数理论值(46.01%);As/S原子比值在0.65~0.94之间,同样低于标准毒砂的As/S原子比值(1:1)。此外,金在含砷黄铁矿和毒砂中分布无环带规律,整体上看,单颗粒毒砂中的金质量分数与含砷黄铁矿中的金质量分数相当。

对载金硫化物电子探针波谱数据分析显示,As与S具有明显的负相关关系(图5A、B),表明As替代S进入黄铁矿和毒砂的晶体结构中,而Au与As之间不是简单的线性关系(图5C)。由Reich等^[4]确定的Au在含砷黄铁矿中的溶解度极限($C_{\text{Au}} = 0.02 \times C_{\text{As}} + 4 \times 10^{-5}$)确定出绝大部分数据点落在溶解度曲线的下方,即 Au^+ 的区域,表明进入载金矿物的Au主要是以不可见的化学结合态金(Au^+)的形式存在,极少数黄铁矿颗粒中为纳米金和结合态金共存。而所有数据点均落在Au:As比值1:100附近,这与Su等^[24]对水银洞金矿床成矿期黄铁矿测得的Au:As比值相似。Deditius等^[23]认为Au:As比值1:100可能代表早期成矿流体中Au的饱和状态,在含砷黄铁矿沉淀的过程中携带大量的金沉淀,致使成矿期流体中Au质量分数的降低。此外,含砷黄铁矿中的As与Fe之间具有较弱的负相关关系(图5D),这与Deditius等^[23]提到的Yanacocha金矿床中部分黄铁矿的As与Fe具有负相关关系类似,表明少部分As可替代Fe进入黄铁矿晶体结构中。

选择有代表性的含金硫化物颗粒进行As、Au、Fe、S和Ti元素的电子探针面扫描分析,其结果见图6。与沉积岩容矿的卡林型金矿(如水银洞金矿床^[25])不同,八渡金矿床中含砷黄铁矿没有环带结构(图6B、H),As在含砷黄铁



Py-Pyrite; Apy-Arsenopyrite; Rt-Rutile; Ill-Illite; Dol-Dolomite; Ap-Apatite; Brt-Barite; Qz-Quartz (A-背散射图像中黄铁矿 (Py) 和毒砂 (Apy) 围绕粒状金红石 (Rt) 共生的关系, 数值为波谱测点的金质量分数 (下同); (B-含金硫化物黄铁矿和毒砂中金质量分数以及蚀变产物伊利石 (Ill) 和白云石 (Dol)); (C-含金硫化物围绕长条状金红石共生的关系; (D-蚀变产物伊利石 (Ill) 充填于粒状金红石空隙中; (E) 矿石中的重晶石脉 (Brt)

图 4 广西八渡金矿床含砷黄铁矿、毒砂的背散射图像

Fig. 4. Backscattered electron images of arsenian pyrite and arsenopyrite from Badu gold deposit in Guangxi.

表 1 广西八渡金矿床含砷黄铁矿的电子探针分析结果($w_B/\%$)

Table 1. Electron probe microanalysis results (wt.%) for arsenian pyrite from Badu gold deposit in Guangxi

Sample	S (0.05)	Fe (0.03)	As (0.03)	Ag (0.03)	Au (0.03)	Se (0.01)	Ni (0.03)	Co (0.03)	Sb (0.03)	Te (0.03)	Hg (0.05)	Total
bd-3	51.67	45.43	3.57	n.d.	0.03	n.d.	n.d.	n.d.	n.d.	n.d.	n.d.	100.71
bd-5	51.43	45.34	4.14	b.d.	b.d.	n.d.	b.d.	n.d.	n.d.	0.06	n.d.	101.01
bd-7	51.39	44.57	4.36	n.d.	n.d.	0.05	b.d.	n.d.	n.d.	n.d.	n.d.	100.37
bd-11	52.35	45.09	3.69	b.d.	0.04	n.d.	0.03	n.d.	b.d.	n.d.	n.d.	101.21
bd-17	50.48	44.11	5.72	n.d.	0.03	n.d.	b.d.	n.d.	n.d.	b.d.	0.07	100.43
bd-18	49.44	43.27	5.17	b.d.	0.06	n.d.	b.d.	n.d.	n.d.	b.d.	n.d.	98.00
bd-23	50.72	43.42	3.70	b.d.	n.d.	0.01	b.d.	n.d.	b.d.	n.d.	b.d.	97.88
bd-25	51.91	43.42	3.24	b.d.	b.d.	0.01	b.d.	n.d.	n.d.	n.d.	n.d.	98.61
bd-26	51.59	44.73	3.23	b.d.	n.d.	n.d.	b.d.	n.d.	n.d.	n.d.	n.d.	99.58
bd-28	53.36	44.85	1.65	n.d.	b.d.	b.d.	0.05	n.d.	b.d.	0.04	b.d.	100.02
bd-29	52.82	45.29	1.61	b.d.	n.d.	0.03	n.d.	n.d.	n.d.	n.d.	b.d.	99.78
bd-31	51.61	45.08	3.11	0.04	0.11	0.01	n.d.	n.d.	b.d.	n.d.	n.d.	99.95
bd-33	51.60	45.28	2.15	b.d.	n.d.	n.d.	0.03	n.d.	n.d.	b.d.	n.d.	99.09
bd-34	50.44	44.27	3.72	n.d.	b.d.	n.d.	0.05	n.d.	n.d.	0.05	0.07	98.61
bd-35	50.66	44.74	3.54	n.d.	b.d.	b.d.	b.d.	n.d.	n.d.	n.d.	n.d.	98.96
bd-37	51.63	45.26	2.53	b.d.	0.03	b.d.	0.05	b.d.	n.d.	n.d.	n.d.	99.53
bd-40	51.53	45.29	3.24	b.d.	n.d.	n.d.	b.d.	n.d.	n.d.	n.d.	n.d.	100.10
bd-41	49.27	43.35	4.82	b.d.	b.d.	0.01	b.d.	n.d.	b.d.	n.d.	n.d.	97.48
bd-42	51.61	44.85	2.81	b.d.	b.d.	n.d.	b.d.	n.d.	n.d.	0.07	n.d.	99.39
bd-43	48.51	42.97	4.36	n.d.	0.07	n.d.	b.d.	n.d.	n.d.	n.d.	b.d.	95.92
bd-44	48.48	43.49	7.41	n.d.	n.d.	0.01	0.09	n.d.	b.d.	n.d.	b.d.	99.51
bd-46	52.68	45.15	1.39	n.d.	0.07	n.d.	b.d.	n.d.	b.d.	n.d.	n.d.	99.30
bd-48	51.10	42.89	2.84	n.d.	0.06	0.04	b.d.	n.d.	n.d.	0.09	n.d.	97.03
bd-53	52.36	45.00	0.56	b.d.	0.06	n.d.	0.04	n.d.	n.d.	b.d.	n.d.	98.03
bd-54	53.47	45.53	0.70	n.d.	b.d.	0.01	b.d.	n.d.	b.d.	b.d.	b.d.	99.76
bd-55	52.96	44.09	0.63	b.d.	0.08	n.d.	n.d.	n.d.	b.d.	0.03	b.d.	97.81
bd-59	48.96	43.10	5.24	b.d.	0.08	n.d.	n.d.	n.d.	n.d.	0.05	b.d.	97.48
bd-67	51.98	45.24	2.88	n.d.	n.d.	n.d.	b.d.	n.d.	b.d.	n.d.	b.d.	100.13
bd-74	47.23	42.24	9.16	b.d.	0.17	0.01	b.d.	n.d.	n.d.	n.d.	n.d.	98.84
bd-77	51.17	44.72	3.33	n.d.	0.03	n.d.	n.d.	n.d.	b.d.	0.04	n.d.	99.31
bd-83	50.72	44.76	4.80	0.04	n.d.	n.d.	b.d.	n.d.	n.d.	n.d.	n.d.	100.34
bd-86	50.70	44.28	4.65	b.d.	n.d.	n.d.	n.d.	n.d.	n.d.	0.05	0.07	99.76
bd-90	50.65	45.73	2.19	n.d.	n.d.	0.02	n.d.	n.d.	n.d.	n.d.	n.d.	98.59
bd-94	51.96	45.97	2.59	n.d.	b.d.	0.02	b.d.	n.d.	n.d.	n.d.	n.d.	100.55
bd-95	50.50	45.68	3.89	b.d.	0.04	0.01	b.d.	b.d.	n.d.	0.03	b.d.	100.18
bd-96	51.93	45.87	1.35	b.d.	0.09	0.01	b.d.	0.03	n.d.	n.d.	b.d.	99.29
bd-97	51.70	46.10	2.15	b.d.	n.d.	0.02	0.05	n.d.	n.d.	n.d.	n.d.	100.02
bd-98	51.57	44.75	2.03	b.d.	n.d.	n.d.	0.07	0.03	b.d.	b.d.	n.d.	98.46
bd-99	52.44	45.49	1.47	n.d.	0.04	n.d.	0.03	n.d.	b.d.	n.d.	n.d.	99.46
bd-100	51.18	44.94	2.61	b.d.	b.d.	0.01	b.d.	n.d.	n.d.	n.d.	n.d.	98.77
bd-101	51.39	45.82	1.78	n.d.	0.03	0.01	b.d.	n.d.	n.d.	n.d.	b.d.	99.08
bd-102	48.68	44.92	5.55	0.03	n.d.	n.d.	b.d.	n.d.	n.d.	0.04	0.06	99.29
bd-103	49.26	44.13	5.25	b.d.	0.07	n.d.	0.10	b.d.	0.04	n.d.	b.d.	98.86
bd-104	49.33	44.60	4.84	b.d.	n.d.	n.d.	0.04	n.d.	b.d.	b.d.	0.06	98.91
bd-105	47.46	43.23	8.06	0.04	n.d.	n.d.	0.05	n.d.	b.d.	0.03	0.06	98.95
bd-106	49.03	44.61	5.59	n.d.	n.d.	n.d.	n.d.	n.d.	b.d.	n.d.	n.d.	99.25
bd-107	52.47	45.86	1.48	n.d.	0.08	n.d.	b.d.	n.d.	b.d.	n.d.	b.d.	99.91
bd-108	52.15	45.95	1.67	b.d.	0.05	n.d.	0.05	0.05	n.d.	n.d.	n.d.	99.94

续表 1

Sample	S (0.05)	Fe (0.03)	As (0.03)	Ag (0.03)	Au (0.03)	Se (0.01)	Ni (0.03)	Co (0.03)	Sb (0.03)	Te (0.03)	Hg (0.05)	Total
bd-109	52.08	46.04	1.47	n.d.	0.05	n.d.	b.d.	n.d.	b.d.	b.d.	n.d.	99.67
bd-110	51.78	45.75	2.57	b.d.	n.d.	n.d.	0.03	n.d.	n.d.	n.d.	n.d.	100.13
bd-111	51.34	44.92	1.79	n.d.	n.d.	n.d.	0.03	b.d.	n.d.	0.03	0.05	98.16
bd-112	50.27	45.34	4.29	0.03	n.d.	n.d.	b.d.	n.d.	b.d.	0.04	n.d.	100.01
bd-114	52.64	45.91	1.49	b.d.	n.d.	n.d.	b.d.	n.d.	n.d.	0.03	b.d.	100.13
bd-115	51.00	44.54	2.54	0.04	0.08	0.03	0.08	n.d.	b.d.	b.d.	b.d.	98.33
bd-116	51.63	45.74	1.63	b.d.	0.05	0.01	0.03	n.d.	n.d.	0.06	n.d.	99.15
bd-117	49.59	43.52	5.28	b.d.	0.10	n.d.	0.05	n.d.	n.d.	0.03	n.d.	98.60
bd-118	49.94	44.94	4.60	b.d.	n.d.	b.d.	0.04	b.d.	n.d.	0.04	b.d.	99.60
bd-119	50.98	44.38	3.38	n.d.	0.03	n.d.	0.04	b.d.	b.d.	n.d.	b.d.	98.86
bd-120	50.47	45.26	3.03	b.d.	0.05	n.d.	0.05	n.d.	n.d.	b.d.	n.d.	98.90
bd-121	50.08	44.66	3.64	n.d.	0.05	0.03	b.d.	n.d.	n.d.	b.d.	n.d.	98.47
bd-122	51.58	45.38	1.50	n.d.	0.03	0.03	b.d.	n.d.	n.d.	b.d.	b.d.	98.55
bd-123	50.88	43.67	4.52	0.03	b.d.	n.d.	0.06	n.d.	b.d.	b.d.	n.d.	99.18
bd-124	51.84	45.20	1.32	b.d.	0.04	n.d.	b.d.	n.d.	n.d.	0.03	n.d.	98.46
bd-125	50.66	44.55	4.17	b.d.	n.d.	n.d.	0.03	n.d.	b.d.	n.d.	b.d.	99.42
bd-129	48.57	43.95	5.34	b.d.	0.03	n.d.	0.06	b.d.	n.d.	n.d.	0.06	98.04
bd-132	49.92	42.73	5.95	b.d.	0.07	n.d.	0.03	n.d.	n.d.	b.d.	0.05	98.79
bd-134	50.58	43.30	3.82	b.d.	n.d.	0.01	b.d.	n.d.	n.d.	n.d.	n.d.	97.74
bd-136	48.05	43.84	6.99	b.d.	0.06	n.d.	0.03	n.d.	b.d.	0.03	n.d.	99.01
bd-141	49.34	44.73	5.18	b.d.	0.06	n.d.	b.d.	n.d.	n.d.	n.d.	n.d.	99.35
bd-144	50.45	45.40	3.47	n.d.	n.d.	0.03	b.d.	n.d.	n.d.	n.d.	n.d.	99.37
bd-147	50.78	44.17	4.34	n.d.	n.d.	0.01	b.d.	n.d.	n.d.	n.d.	b.d.	99.35
bd-153	51.13	45.20	3.31	0.03	0.05	n.d.	n.d.	n.d.	b.d.	n.d.	n.d.	99.72
bd-154	51.84	43.20	4.34	n.d.	n.d.	n.d.	b.d.	n.d.	b.d.	b.d.	n.d.	99.41
bd-155	51.04	45.37	2.85	n.d.	n.d.	n.d.	b.d.	n.d.	n.d.	n.d.	n.d.	99.28
bd-156	51.75	45.16	2.19	n.d.	n.d.	n.d.	n.d.	n.d.	n.d.	n.d.	n.d.	99.10
bd-169	50.86	44.66	2.42	n.d.	0.03	0.01	0.09	b.d.	n.d.	n.d.	b.d.	98.11
bd-173	50.63	44.17	2.42	b.d.	0.03	n.d.	b.d.	n.d.	n.d.	0.03	n.d.	97.29
bd-175	51.11	44.84	3.27	0.03	0.03	0.02	b.d.	n.d.	n.d.	b.d.	n.d.	99.32
bd-177	51.11	45.31	3.13	b.d.	n.d.	n.d.	n.d.	n.d.	b.d.	n.d.	b.d.	99.59
bd-178	50.80	45.42	2.79	b.d.	0.07	n.d.	0.03	n.d.	n.d.	n.d.	b.d.	99.13
bd-180	50.69	45.73	3.49	n.d.	n.d.	n.d.	n.d.	n.d.	n.d.	0.05	n.d.	99.95
bd-182	52.18	45.13	2.74	0.04	0.09	0.05	n.d.	n.d.	n.d.	b.d.	n.d.	100.24
bd-184	51.59	44.76	2.75	b.d.	n.d.	n.d.	0.03	n.d.	n.d.	n.d.	b.d.	99.14
bd-188	51.34	44.85	2.15	b.d.	b.d.	0.04	b.d.	n.d.	0.03	b.d.	n.d.	98.44
bd-189	51.44	45.10	2.24	n.d.	0.10	n.d.	b.d.	n.d.	n.d.	n.d.	n.d.	98.88
bd-190	51.94	45.42	2.66	b.d.	0.11	n.d.	b.d.	n.d.	n.d.	n.d.	b.d.	100.18
bd-191	50.28	44.69	2.86	b.d.	n.d.	n.d.	n.d.	n.d.	n.d.	b.d.	b.d.	97.86
bd-192	51.75	44.49	2.91	b.d.	n.d.	0.01	n.d.	n.d.	n.d.	n.d.	n.d.	99.15
bd-194	51.52	44.09	2.04	b.d.	0.04	n.d.	b.d.	n.d.	b.d.	n.d.	b.d.	97.72
bd-196	51.82	44.69	2.53	n.d.	0.04	n.d.	n.d.	n.d.	0.03	n.d.	0.07	99.17
bd-198	52.33	44.37	2.65	b.d.	n.d.	n.d.	b.d.	n.d.	b.d.	b.d.	n.d.	99.40

注: b.d.-低于检出限 (below detectable limit); n. d.-未检测到 (not detected).

矿中均匀分布, 暗示整个黄铁矿颗粒是同时期热液成因的。面扫描中金分布不明显, 暗示与卡林型金矿 (如水银洞金矿床^[25]) 相比金质量分

数更低。硫化物中 As 与 S 具有相互消长的对应关系(图 6H、K), 这与图 5A 中 As 与 S 的关系图一致, 表明 As 替代 S 进入黄铁矿结构中。Ti

表 2 广西八渡金矿床毒砂的电子探针分析结果 ($w_B/\%$)

Table 2. Electron probe microanalysis results (wt.%) for arsenopyrite from Badu gold deposit in Guangxi

Sample	S (0.05)	Fe (0.03)	As (0.03)	Ag (0.03)	Au (0.03)	Se (0.01)	Ni (0.03)	Co (0.03)	Sb (0.03)	Te (0.03)	Hg (0.05)	Total
bd-1	22.21	33.96	46.27	b.d.	n.d.	n.d.	b.d.	n.d.	n.d.	b.d.	n.d.	102.47
bd-2	21.84	34.51	46.19	b.d.	0.10	n.d.	n.d.	n.d.	b.d.	0.03	n.d.	102.68
bd-4	22.99	34.58	44.09	n.d.	b.d.	n.d.	0.03	n.d.	n.d.	n.d.	n.d.	101.71
bd-6	22.09	33.94	46.39	0.03	n.d.	n.d.	0.03	b.d.	b.d.	0.03	b.d.	102.57
bd-8	21.11	34.18	45.59	b.d.	0.05	n.d.	b.d.	n.d.	b.d.	b.d.	0.07	101.05
bd-9	22.90	34.47	45.12	b.d.	n.d.	n.d.	0.04	n.d.	n.d.	b.d.	b.d.	102.59
bd-10	22.04	33.40	47.11	b.d.	n.d.	n.d.	b.d.	n.d.	n.d.	n.d.	b.d.	102.62
bd-12	22.88	32.94	44.68	b.d.	b.d.	n.d.	0.03	n.d.	n.d.	n.d.	0.06	100.63
bd-13	21.91	33.34	45.49	n.d.	0.09	n.d.	b.d.	b.d.	n.d.	b.d.	b.d.	100.90
bd-14	23.43	33.74	45.43	n.d.	n.d.	n.d.	b.d.	n.d.	n.d.	n.d.	b.d.	102.63
bd-15	22.8	34.33	44.44	0.03	0.11	n.d.	b.d.	n.d.	n.d.	n.d.	b.d.	101.77
bd-16	22.21	33.35	46.47	n.d.	0.05	n.d.	0.04	n.d.	n.d.	n.d.	b.d.	102.12
bd-19	22.96	33.93	44.72	b.d.	0.14	n.d.	n.d.	n.d.	b.d.	b.d.	b.d.	101.81
bd-20	21.53	33.74	44.41	n.d.	n.d.	n.d.	b.d.	n.d.	n.d.	n.d.	b.d.	99.70
bd-21	24.59	34.69	41.99	n.d.	n.d.	n.d.	b.d.	n.d.	n.d.	n.d.	b.d.	101.30
bd-24	21.91	33.30	46.55	b.d.	0.03	n.d.	b.d.	n.d.	n.d.	b.d.	b.d.	101.82
bd-30	21.13	34.57	45.65	n.d.	0.07	n.d.	n.d.	n.d.	b.d.	n.d.	b.d.	101.46
bd-38	22.12	33.71	45.40	b.d.	0.12	n.d.	b.d.	n.d.	n.d.	n.d.	n.d.	101.37
bd-39	23.39	34.48	44.03	n.d.	0.03	n.d.	b.d.	n.d.	n.d.	b.d.	b.d.	101.97
bd-45	22.34	33.71	44.57	n.d.	0.04	n.d.	n.d.	n.d.	b.d.	0.04	0.05	100.76
bd-47	22.07	34.12	46.28	n.d.	n.d.	n.d.	n.d.	n.d.	n.d.	n.d.	n.d.	102.47
bd-49	22.97	34.32	44.65	n.d.	0.04	n.d.	n.d.	n.d.	n.d.	n.d.	n.d.	101.98
bd-50	22.73	32.42	44.34	0.03	0.07	n.d.	n.d.	n.d.	b.d.	b.d.	n.d.	99.60
bd-51	21.96	33.07	45.96	b.d.	0.14	n.d.	n.d.	n.d.	n.d.	0.07	n.d.	101.21
bd-64	24.36	34.67	41.89	n.d.	b.d.	n.d.	n.d.	n.d.	b.d.	b.d.	n.d.	100.94
bd-65	23.56	32.17	43.70	b.d.	0.03	n.d.	b.d.	n.d.	b.d.	n.d.	n.d.	99.47
bd-66	23.29	33.55	42.28	b.d.	b.d.	n.d.	b.d.	n.d.	n.d.	n.d.	0.05	99.21
bd-68	22.15	33.25	43.20	n.d.	0.10	n.d.	n.d.	n.d.	b.d.	0.03	0.08	98.82
bd-69	25.77	35.16	39.55	b.d.	n.d.	n.d.	0.03	n.d.	n.d.	n.d.	b.d.	100.56
bd-70	23.47	34.22	44.04	n.d.	n.d.	n.d.	b.d.	n.d.	n.d.	n.d.	n.d.	101.74
bd-71	24.42	33.90	41.79	n.d.	0.04	n.d.	0.07	n.d.	n.d.	b.d.	n.d.	100.21
bd-75	23.34	33.69	42.43	n.d.	b.d.	n.d.	n.d.	n.d.	n.d.	n.d.	n.d.	99.47
bd-76	22.11	34.11	45.06	b.d.	0.04	n.d.	b.d.	n.d.	n.d.	n.d.	n.d.	101.33
bd-79	22.10	33.11	44.02	n.d.	n.d.	n.d.	b.d.	n.d.	n.d.	n.d.	0.08	99.33
bd-82	24.47	34.22	42.29	b.d.	n.d.	n.d.	b.d.	n.d.	n.d.	n.d.	b.d.	100.98
bd-84	22.52	33.69	44.55	n.d.	n.d.	n.d.	n.d.	n.d.	b.d.	n.d.	n.d.	100.76
bd-85	22.19	34.07	44.97	b.d.	n.d.	n.d.	b.d.	n.d.	n.d.	0.04	n.d.	101.30
bd-87	23.45	34.23	42.07	b.d.	0.05	n.d.	b.d.	n.d.	n.d.	0.05	n.d.	99.86
bd-88	22.25	33.76	45.29	n.d.	0.04	n.d.	b.d.	n.d.	b.d.	0.05	0.06	101.45
bd-89	22.13	34.05	44.19	b.d.	b.d.	n.d.	b.d.	n.d.	n.d.	b.d.	n.d.	100.39
bd-92	21.82	33.99	46.41	0.03	n.d.	n.d.	b.d.	n.d.	n.d.	n.d.	b.d.	102.32
bd-93	22.74	34.14	45.11	0.03	n.d.	n.d.	n.d.	n.d.	n.d.	b.d.	b.d.	102.04
bd-126	22.92	33.97	42.85	b.d.	n.d.	n.d.	b.d.	n.d.	n.d.	n.d.	n.d.	99.76
bd-127	23.47	33.67	42.08	b.d.	n.d.	n.d.	b.d.	n.d.	b.d.	0.07	b.d.	99.33
bd-128	23.48	34.37	43.09	n.d.	b.d.	n.d.	n.d.	n.d.	b.d.	n.d.	b.d.	100.97
bd-130	22.96	33.92	42.99	n.d.	n.d.	n.d.	n.d.	n.d.	n.d.	n.d.	n.d.	99.88
bd-131	23.03	34.24	42.41	n.d.	n.d.	n.d.	b.d.	n.d.	n.d.	b.d.	n.d.	99.69
bd-133	23.83	34.08	40.91	b.d.	0.05	n.d.	0.03	n.d.	n.d.	n.d.	b.d.	98.93

续表 2

Sample	S (0.05)	Fe (0.03)	As (0.03)	Ag (0.03)	Au (0.03)	Se (0.01)	Ni (0.03)	Co (0.03)	Sb (0.03)	Te (0.03)	Hg (0.05)	Total
bd-135	23.48	34.52	43.16	n.d.	n.d.	n.d.	0.03	b.d.	b.d.	b.d.	n.d.	101.21
bd-137	24.14	33.31	40.77	b.d.	n.d.	n.d.	0.04	b.d.	n.d.	b.d.	b.d.	98.30
bd-138	22.41	33.80	44.87	n.d.	b.d.	n.d.	n.d.	n.d.	n.d.	b.d.	n.d.	101.11
bd-139	24.77	34.57	41.75	n.d.	n.d.	n.d.	b.d.	n.d.	b.d.	n.d.	b.d.	101.12
bd-140	22.05	33.54	43.00	b.d.	n.d.	n.d.	b.d.	n.d.	n.d.	n.d.	n.d.	98.61
bd-142	22.35	34.38	45.62	b.d.	0.09	n.d.	n.d.	n.d.	n.d.	0.03	b.d.	102.48
bd-143	23.37	34.27	42.04	n.d.	n.d.	n.d.	n.d.	n.d.	n.d.	0.06	0.05	99.80
bd-145	22.03	34.12	43.35	b.d.	0.03	n.d.	0.03	n.d.	n.d.	b.d.	n.d.	99.60
bd-146	23.08	33.21	41.79	n.d.	n.d.	n.d.	b.d.	n.d.	n.d.	b.d.	0.05	98.16
bd-150	23.61	34.61	43.52	n.d.	0.03	n.d.	b.d.	n.d.	n.d.	b.d.	n.d.	101.77
bd-151	22.20	34.29	43.23	b.d.	b.d.	n.d.	b.d.	b.d.	n.d.	0.05	n.d.	99.79
bd-152	24.62	33.06	40.63	b.d.	n.d.	n.d.	b.d.	n.d.	b.d.	0.05	n.d.	98.42
bd-157	21.64	33.93	45.24	n.d.	0.04	n.d.	n.d.	n.d.	n.d.	n.d.	0.09	100.95
bd-158	23.29	33.94	40.87	b.d.	n.d.	n.d.	b.d.	n.d.	b.d.	0.03	n.d.	98.17
bd-159	21.53	34.24	45.25	b.d.	0.03	n.d.	b.d.	n.d.	b.d.	0.03	b.d.	101.13
bd-160	21.17	34.04	44.95	b.d.	n.d.	n.d.	n.d.	n.d.	n.d.	b.d.	b.d.	100.19
bd-161	21.53	34.21	46.31	n.d.	0.05	n.d.	0.08	b.d.	n.d.	b.d.	n.d.	102.20
bd-162	21.55	34.25	46.47	n.d.	0.10	n.d.	b.d.	n.d.	b.d.	n.d.	n.d.	102.40
bd-163	21.17	33.50	45.06	n.d.	0.14	n.d.	b.d.	n.d.	n.d.	b.d.	n.d.	99.90
bd-165	22.45	33.75	43.75	b.d.	0.04	n.d.	b.d.	n.d.	n.d.	0.03	n.d.	100.05
bd-166	21.88	33.89	45.32	n.d.	n.d.	n.d.	n.d.	n.d.	n.d.	b.d.	b.d.	101.13
bd-167	21.12	33.78	45.73	n.d.	b.d.	n.d.	b.d.	n.d.	n.d.	0.03	n.d.	100.68
bd-168	22.45	34.20	44.72	n.d.	n.d.	n.d.	0.07	b.d.	0.03	0.03	n.d.	101.51
bd-170	22.21	34.33	42.91	b.d.	0.09	n.d.	0.06	b.d.	b.d.	n.d.	0.06	99.72
bd-171	20.43	33.24	45.24	n.d.	n.d.	n.d.	b.d.	n.d.	n.d.	0.03	0.08	99.03
bd-172	22.20	34.51	43.72	b.d.	0.15	n.d.	b.d.	n.d.	0.03	n.d.	n.d.	100.63
bd-174	21.34	33.68	44.83	b.d.	b.d.	n.d.	b.d.	n.d.	b.d.	0.09	b.d.	100.04
bd-176	21.68	34.52	45.47	n.d.	n.d.	n.d.	n.d.	n.d.	n.d.	n.d.	n.d.	101.67
bd-185	23.07	34.73	43.75	b.d.	n.d.	n.d.	b.d.	n.d.	n.d.	n.d.	b.d.	101.60
bd-186	22.02	34.09	44.92	n.d.	0.05	n.d.	n.d.	n.d.	n.d.	0.04	n.d.	101.12
bd-193	22.19	34.17	43.32	n.d.	0.05	n.d.	n.d.	n.d.	n.d.	b.d.	b.d.	99.75
bd-195	22.37	34.30	45.70	n.d.	n.d.	n.d.	n.d.	n.d.	n.d.	b.d.	b.d.	102.38
bd-197	21.63	34.12	42.45	n.d.	0.03	n.d.	0.04	n.d.	n.d.	b.d.	n.d.	98.27
bd-200	22.11	34.58	44.36	b.d.	0.04	n.d.	0.05	n.d.	n.d.	n.d.	0.05	101.21
bd-201	22.32	34.37	40.69	b.d.	b.d.	n.d.	b.d.	n.d.	n.d.	n.d.	n.d.	97.44
bd-202	23.34	34.77	41.15	b.d.	0.03	n.d.	b.d.	n.d.	n.d.	n.d.	b.d.	99.33

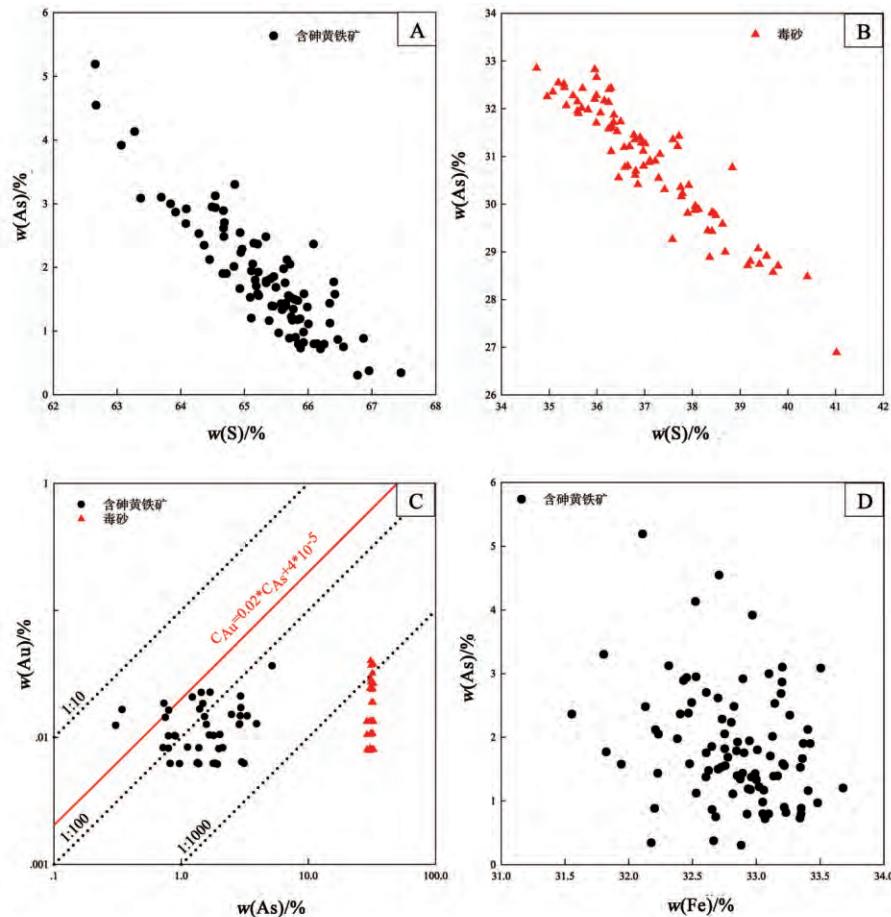
注: b.d.-低于检出限 (below detectable limit); n.d.-未检测到 (not detected).

元素的面扫描显示, 含金硫化物围绕金红石分布 (图 6F、L), 可能表明辉绿岩中含钛辉石或钛铁矿热液蚀变形成金红石, 同时沉淀出含金硫化物共生 (图 6A、G)。

显微镜下观察和电子探针背散射图像显示, 金红石 (TiO_2) 可能是由容矿岩石辉绿岩中的含钛辉石或钛铁矿 (FeTiO_3) 热液蚀变形成, 仅残留钛铁矿晶体格架, 形成的大量溶蚀空洞并被粘土矿物 (主要为伊利石) 及碳酸盐矿物 (硅化

白云石等) 充填, 这类热液交代形成的金红石与含金硫化物密切共生, 表明金红石与含金黄铁矿和毒砂属于同一期次的产物。

苏文超^[24, 26]在对黔西南水银洞和丫他卡林型金矿床进行原生矿石显微岩相学结构和含金硫化物矿物学与地球化学研究后认为含 Fe 碳酸盐矿物溶解释放的 Fe 很可能是该类型金矿床含金硫化物中 Fe 的主要来源, 溶解 Fe 的硫化物化过程是该类型金矿床沉淀富集最重要的机制之一。根据本

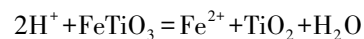
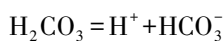
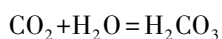


(A-含砷黄铁矿中 As 与 S 的质量分数关系; (B-毒砂中 As 与 S 的质量分数关系; (C) 含砷黄铁矿和毒砂中 Au 与 As 的质量分数关系 (图中红色直线为 Au 在含砷黄铁矿中的溶解度极限^[4], 点线表示 Au: As 比值); (D-含砷黄铁矿中 As 与 Fe 的质量分数关系

图 5 广西八渡金矿床矿石中含砷黄铁矿及毒砂中 Au、S、Fe 和 As 的质量分数关系图
Fig. 5. Correlation of As vs. S (A and B), Au vs. As (C) and As vs. Fe (D)
for arsenian pyrite and arsenopyrite in ores from Badu gold deposit in Guangxi.

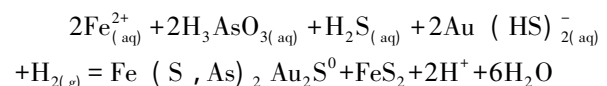
次工作的野外地质观察, 结合原生矿石显微矿相学结构, 含金硫化物 (含砷黄铁矿和毒砂) 的矿物学特征以及围岩蚀变特征, 我们认为八渡金矿床中金的成矿主要经历了以下 2 个过程:

(1) 含铁的钛铁矿溶解 (释放 Fe) 流体包裹体研究显示, 八渡金矿床成矿流体以富含 CO_2 为特征 (待发表)。热力学计算表明, 中低温成矿条件下, 这类富 CO_2 流体属于弱酸性流体, 其 pH 值在 5.07~5.21 之间 (Hofstra 和 Cline^[27]), 这种弱酸性的含 Au 热液可以使赋矿围岩辉绿岩中的含 Ti 辉石或者钛铁矿溶解, 致使 Fe^{2+} 进入含 Au 热液体系, 从而为硫化物过程和金的沉淀富集提供了 Fe 的来源。其化学反应如下:



(2) 溶解 Fe 的硫化物化与金的沉淀富集

热力学与实验地球化学研究表明, 在中低温、富 H_2S 的弱酸性条件下, Au 在流体中主要以 $\text{Au}(\text{HS})_2^-$ 或 $\text{Au}(\text{HS})^0$ 的形式迁移^[28,29], 而 As 则主要以 H_3AsO_3 的形式存在^[30,31]。在相对还原的条件下 (如赋矿围岩中含有机质或煤等), 溶解 Fe^{2+} 的硫化物化形成含砷黄铁矿 ($\text{Fe}[\text{S}, \text{As}]_2$) 和黄铁矿 ($\text{Fe}[\text{S}]_2$), 使 Au 可能以化学结合态 (Au^+) 的形式进入含砷黄铁矿结构中。其化学反应可能为:



如上所述, 含钛辉石或钛铁矿蚀变溶解释放出 Fe, 硫化物化过程沉淀金的同时, 钛铁矿因

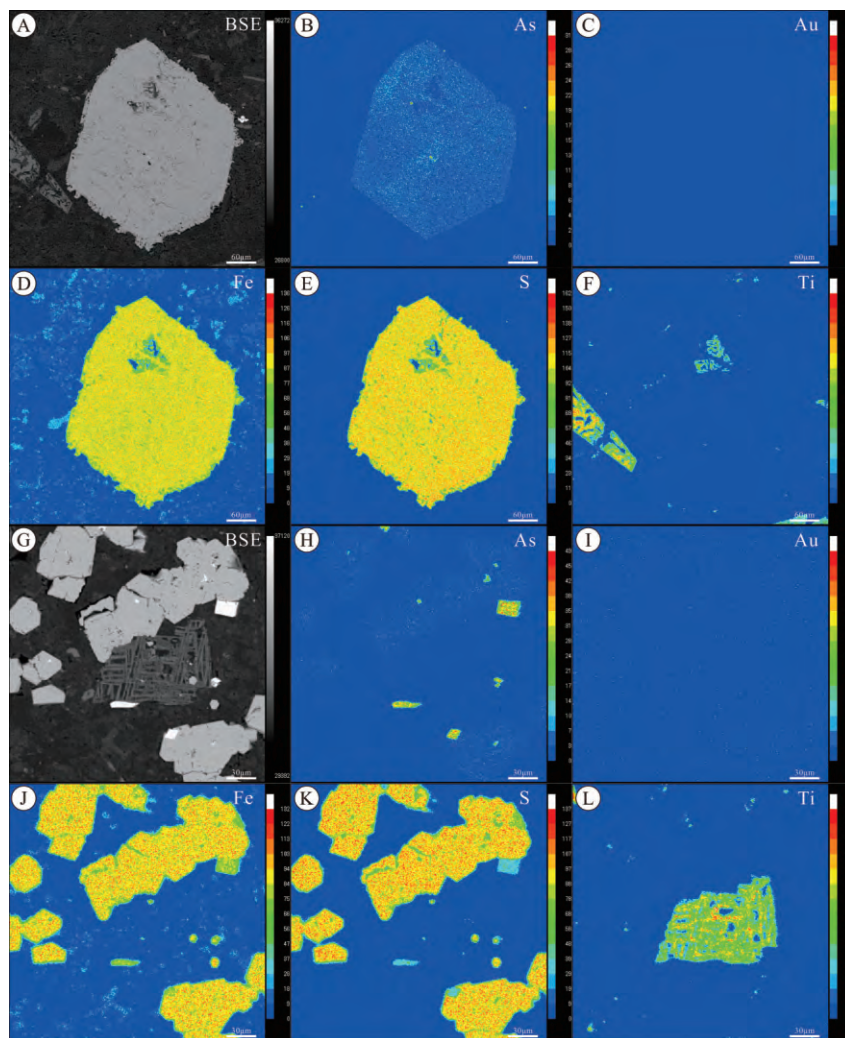


图6 广西八渡金矿床矿石中含金硫化物电子探针背散射图像和 As、Au、Fe、S 和 Ti 的面分布图
Fig. 6. EPMA-BSE images of gold-bearing sulfides and maps of arsenic, gold, iron, sulfur and titanium in ores from Badu gold deposit in Guangxi

丢失 Fe 而变为 TiO_2 (金红石), 并保留钛铁矿原始晶体结构的形态, 因而与含金硫化物密切共生 (图 4A、C、D)。

6 结论

(1) 八渡金矿床中, 黄铁矿和毒砂是最主要的载金矿物, 黄铁矿为含砷黄铁矿, 但未见富砷环带。

(2) 毒砂中的金质量分数比含砷黄铁矿中的略高, 进入载金矿物的 Au 主要是以不可见的化学结合态金 (Au^+) 的形式存在。面分析显示含砷黄铁矿无环带结构, Au 质量分数很低, 含金硫化物多围绕金红石分布。

(3) 金红石是由辉绿岩中的钛铁矿热液蚀变形成, 保留钛铁矿晶体格架, 形成的大量溶蚀空洞被粘土矿物及碳酸盐矿物充填, 热液交代形成的金红石与含金硫化物密切共生, 指示出金红石与含金黄铁矿和毒砂是同一期次的产物。

(4) 八渡金矿床成矿作用的过程为: 赋矿围岩辉绿岩中含钛辉石或钛铁矿的蚀变溶解为金的矿化提供 Fe; 硫化物化过程形成了含 Au 的含砷黄铁矿和毒砂; 保留钛铁矿和含钛辉石晶体形态的金红石与含金硫化物密切共生。

致谢: 室内测试分析得到中国科学院地球化学研究所矿床地球化学国家重点实验室郑文勤老师的帮助, 在此表示衷心的感谢!

参 考 文 献:

- [1] Bowell R J, Baumann M, Gingrich M, Tretbar D, Perkins W F, Fisher P C. The occurrence of gold at the Getchell mine, Nevada [J]. *Journal of Geochemical Exploration*, 1999, 67: 127-143.
- [2] Simon G, Kesler S, Chryssoulis S. Geochemistry and textures of gold-bearing arsenian pyrite, Twin Creeks, Nevada: Implications for deposition of gold in Carlin-type deposit [J]. *Economic Geology*, 1999, 94: 405-422.
- [3] Palenik C S, Utsunomiya S, Reich M. "Invisible" gold revealed: Direct imaging of gold nanoparticles in a Carlin-type gold deposit [J]. *American Mineralogist*, 2004, 89: 1359-1366.
- [4] Reich M, Kesler S, Utsunomiya S, Palenik C S, Chryssoulis S L, Ewing R C. Solubility of gold in arsenic pyrite [J]. *Geochimica et Cosmochimica Acta*, 2005, 69(11): 2781-2796.
- [5] Cline J S, Hofstra A H, Muntean J L, Tosdal R M, Hickey K A. Carlin-type gold deposit in Nevada: Critical geologic characteristics and viable model [J]. *Economic Geology*. 100th Anniversary Volume, 2005, 451-484.
- [6] 张复新, 马建秦, 陈衍景. 秦岭卡林型金矿床金、砷地球化学探讨 [J]. *地球化学*, 1999, 28(5): 453-463.
- [7] 肖龙. 一种新的微细浸染型金矿——产于辉绿岩中的微细浸染型金矿特征及找矿标志 [J]. *地质与勘探*, 1997, 33(6): 1-6.
- [8] 潘家永, 张乾, 邵树勋. 桂西北发现一类新的微细浸染型金矿 [J]. *黄金*, 1998, 19(7): 3-5.
- [9] 覃文明, 何志美. 桂西北与辉绿岩类岩石有关的金矿地质特征——以百色龙川金矿为例 [J]. *黄金地质*, 2003, 9(3): 49-54.
- [10] 吴江, 李思田, 王灿, 李甫安, 谢家盈, 李正海. 桂西北微细粒浸染型金矿成矿作用分析 [J]. *广西地质*, 1993, 6(2): 39-51.
- [11] 国家辉. 桂西北超微粒浸染型金矿成矿地质条件及找矿模式 [J]. *广西地质*, 1994a, 7(2): 37-50.
- [12] 国家辉. 桂西北地区超微粒浸染型金矿标型特征 [J]. *贵金属地质*, 1994b, 3(4): 289-292.
- [13] 国家辉. 桂西北地区超微粒型金矿成矿条件及其成矿预测 [J]. *贵金属地质*, 1994c, 3(3): 200, 233-240.
- [14] 国家辉. 桂西北地区超微粒浸染型金矿氧化矿形成条件及找矿 [J]. *贵金属地质*, 1996, 5(4): 266-278.
- [15] 国家辉. 桂西北地区岩浆活动与超微粒型金矿化的关系 [J]. *贵金属地质*, 2000, 9(3): 133-143.
- [16] 谢世业, 陈大经, 李毅. 桂西北热水沉积型金矿成矿系列、找矿标志及找矿前景 [J]. *地质与勘探*, 2006, 42(3): 12-17.
- [17] 张敏, 庞保成, 吴荣华, 李文龙. 桂西北地区微细粒浸染型金矿地质特征和流体包裹体研究 [J]. *现代矿业*, 2011, (12): 50-52, 85.
- [18] 覃少耀, 颜小东. 广西田林县八渡金矿地质矿化特征及成因研究 [J]. *广东科技*, 2012, 21(19): 140-141, 172.
- [19] 苏文超. 扬子地块西南缘卡林型金矿床的成矿流体地球化学研究 [D]. 贵阳: 中国科学院地球化学研究所 (博士论文), 2002, 1-116.
- [20] Lubben J D, Cline J S, Barker S L L. Ore Fluid Properties and Sources from Quartz-Associated Gold at the Betze-Post Carlin-Type Gold Deposit, Nevada, United States [J]. *Economic Geology*, 2012, 107(7): 1351-1385.
- [21] Su W C, Xia B, Zhang H T, Zhang X C, Hu R Z. Visible gold in arsenian pyrite at the Shuiyindong Carlin-type gold deposit, Guizhou, China: Implications for the environment and processes of ore formation [J]. *Ore Geology Reviews*, 2008, 33(3-4): 667-679.
- [22] 陈懋弘, 毛景文, 陈振宇, 章伟. 滇黔桂“金三角”卡林型金矿含砷黄铁矿和毒砂的矿物学研究 [J]. *矿床地质*, 2009, 28(5): 539-557.
- [23] Deditius A P, Reich M, Kesler S E, Utsunomiya S, Chryssoulis S L, Walshe J, Ewing R C. The coupled geochemistry of Au and As in pyrite from hydrothermal ore deposits. *Geochimica et Cosmochimica Acta*, 2014, 140: 644-670.
- [24] Su W C, Zhang H T, Hu R Z, Ge X, Xia B, Chen Y Y, Zhu C. Mineralogy and geochemistry of gold-bearing arsenian pyrite from the Shuiyindong Carlin-type gold deposit, Guizhou, China: Implications for gold depositional processes [J]. *Mineralium Deposita*, 2012, 47(6): 653-662.
- [25] 张弘弘. 贵州水银洞卡林型金矿床含金硫化物地球化学与金的赋存状态研究 [D]. 贵阳: 中国科学院地球化学研究所 (硕士论文), 2007, 1-88.
- [26] 苏文超. 黔西南卡林型金矿热液化学及其成矿作用 [R]. 广州: 中国科学院广州地球化学研究所 (博士后报告), 2009, 1-80.
- [27] Hofstra A H, Cline J S. Characteristics and models for Carlin-type gold deposits [A]. *Reviews in Economic Geology* [M]. Hagemann S. G. and Brown P. E. (eds) GOLD IN 2000: 163-220.
- [28] Seward T M. Thio complexes of gold and the transport of gold in hydrothermal ore solutions [J]. *Geochimica et Cosmochimica Acta*, 1973, 37(3): 379-399.
- [29] Seward T M. The hydrothermal geochemistry of gold [A]. Foster R P, Eds., Gold metallogeny and exploration. Blackie [M], 1993, 37-62.
- [30] Heinrich C A, Eadington P J. Thermodynamic predictions of the hydrothermal chemistry of arsenic, cassiterite-arsenopyrite-base metal sulfide deposits [J]. *Economic geology*, 1986, 81: 511-529.
- [31] Pokrovski G S, Kara S, Roux J. Stability and solubility of arsenopyrite, FeAsS, in crustal fluids [J]. *Geochimica et Cosmochimica Acta*, 2002, 66(13): 2361-2378.